Swelling and Module Pre-loading Considerations in EV Battery Crash Simulations

Sriram Seshadri[1], Alexis Wilson[1]

[1] Automotive Cells Company – Bruges, 33520 France

1 Introduction

Automotive transportation is currently undergoing a transition away from Internal Combustion Engine (ICE) powered vehicles towards more sustainable propulsion methods. Of the possible approaches, Battery Electric Vehicles is one of the fastest growing markets, with an increase of 26.1% between January-May 2024 and the same period in 2025, against +15% for Plug-In Hybrid Electric Vehicles (PHEV) and 19.8% for Hybrid Electric Vehicles (HEV) [1].

As the use of BEVs increases, the ability to understand and mitigate abusive phenomena, such as thermal propagation, short circuits and electrolyte leakage, is crucial. These events can be triggered by mechanical loads, whether indirectly during a vehicle crash or directly through intrusions into the battery pack.

Explicit Finite Element Analysis (FEA) simulations using Ansys LS-DYNA® are key to predicting mechanical abusive events, their triggering mechanisms and how designs can be improved. Different scales can be considered when developing, and indeed modelling, batteries. The three “typical” product level scales are cell, module (i.e. assembly of cells) and pack (i.e. assembly of modules). For the remainder of this paper, only Nickel Manganese Cobalt (NMC) chemistry based prismatic cell and module scales will be considered.

FEA module models can be developed using cell models assembled through welded / glued connections with a module casing. However, a cell model with good stiffness correlation to crush test data is no guarantee of a similar level of correlation at module level due to for example differences in test boundary conditions (Fig.1: and Fig.2:).

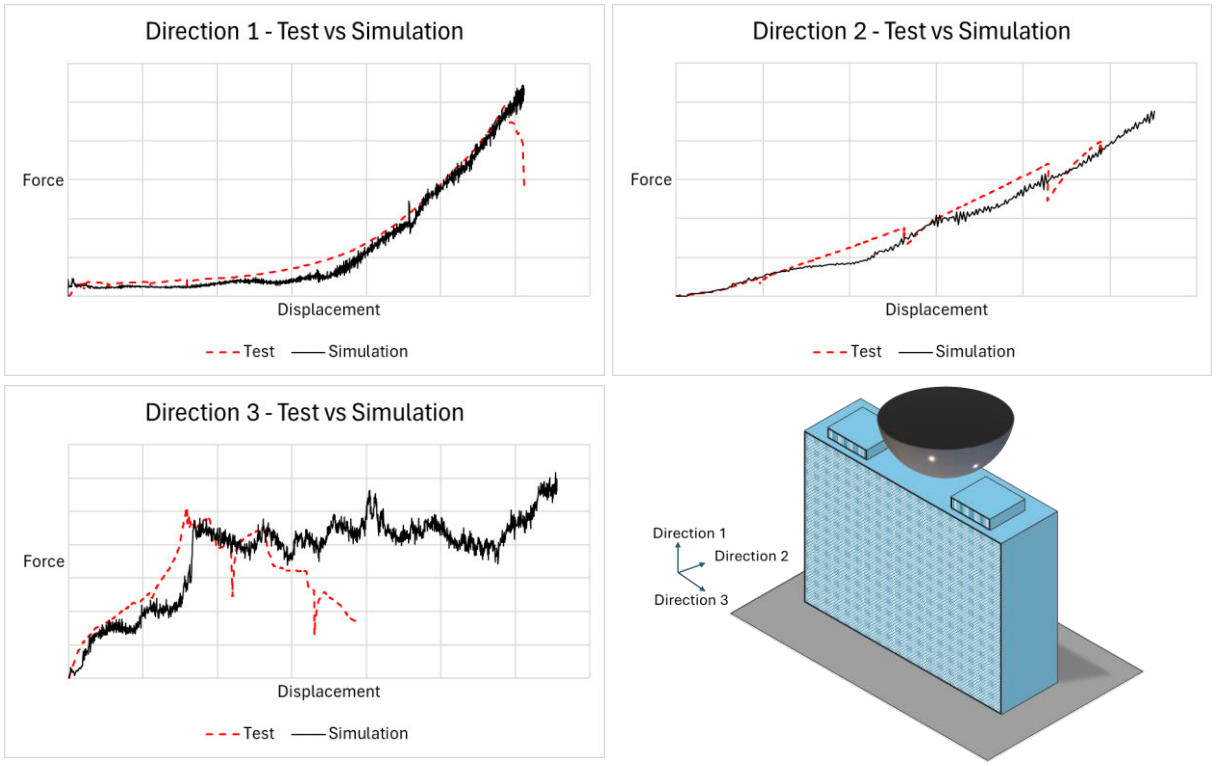

Fig.1: Test and Simulation prismatic cell crush behaviour comparison

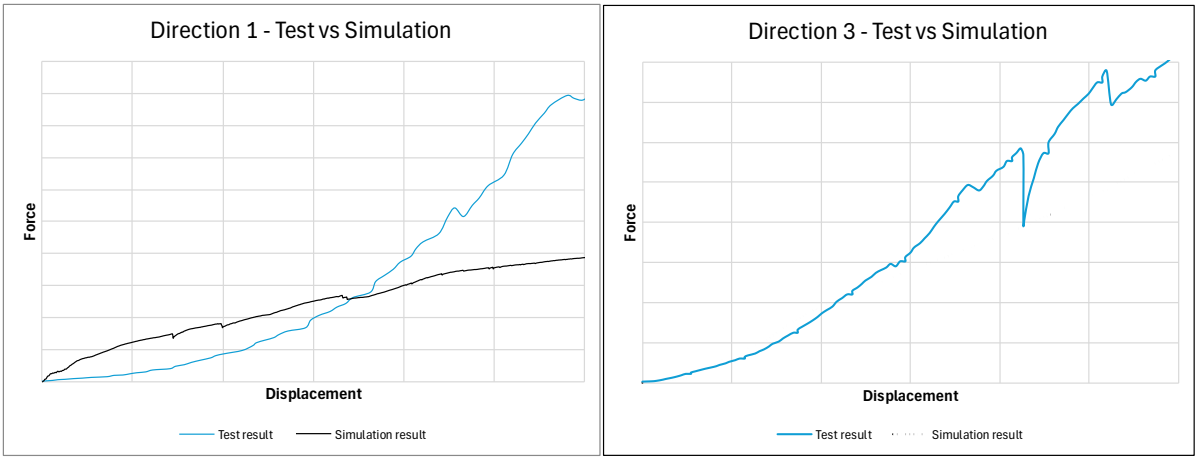

Fig.2: Test and Simulation prismatic cell module crush behaviour comparison

One of the aspects which may affect battery module stiffness and general mechanical behaviour are cell swelling and assembly pre-loads. Cell swelling occurs even at the Beginning of Life (BOL) of a module, due to the electrical formation process and the initial charged state of the cells. Reversible swelling (charging and discharging cycles resulting in the change in State of Charge (SOC) of the cell) is observed due to ion concentration in electrodes i.e. electrodes expand or contract inducing mechanical stress within the cell [2]. Assembly pre-loads occur during the compression of module components and sub-assemblies, where the thermal insulators (TI) undergo large amounts of deformation to reach the nominal module length required. Furthermore, residual forces could be present in welded and glued connections of an assembled module. It is not expected that weld pre-loading on the specific module configuration studies will affect module stiffness, but rather module strength which is not the focus of this study. Therefore this paper will focus on cell swelling and TI compression pre-loading implementation, and their impact on module mechanical safety simulations.

2 General model description

As illustrated in Fig.3: below, an eight cell module configuration is used as the basis for all pre-loading and swelling studies. This section describes the model setup characteristics for the key areas of interest.

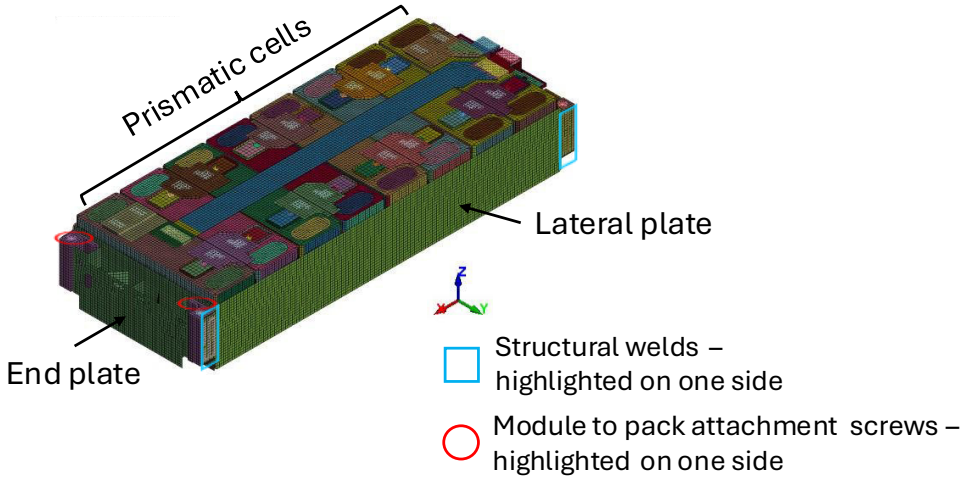

Fig.3: Prismatic cell module Ansys LS-DYNA® model

The cell casing, lateral plates and electrical connections are modelled using shell elements. The endplate is modelled with a mix of 2D and 3D elements, connected with a **`*TIED_SHELL_EDGE_TO_SOLID`** contact. TIs are modelled using 3D elements in all pre-loading methods; however, depending on the method, a 2D null shell coating may be applied for specific contact definitions. The cell stack is modelled using 3D elements in a single, homogeneous block, i.e. homogeneous stack properties are determined from the electrode and separator properties.

The TI stress-strain curve indicates mechanical behaviour close to that of a foam-type material (Fig.4:). Therefore, the TIs are characterised using a **`*MAT_LOW_DENSITY_FOAM`** material model. A **`*MAT_MODIFIED_HONEYCOMB`** material model is used for the cell stack component, which allows for three separate stress-strain curves in each orthogonal direction, and by extension facilitates correlation with data such as that shown in Fig.1:. The metallic components, such as lateral plates and cell casings are modelled with **`*MAT_JOHNSON_COOK`**.

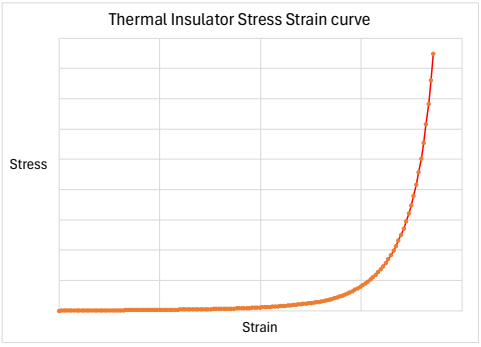

Fig.4: Thermal Insulator Material Stress-Strain Curve

A single surface contact is used for all penalty contact interfaces in the model, with separate contact keywords created depending on the TI compression method. These specific contacts are detailed in Section 3.

3 Module assembly thermal insulator pre-loading

The assembly process of a battery module typically consists of a “stacking” phase, whereby subassemblies and components are compressed to reach the nominal module length. In this example, prismatic cells and TIs are compressed between metallic endplates and when the required length is reached, lateral plates are connected to the stacked components through glueing, welding or a combination of both (Fig.5:)

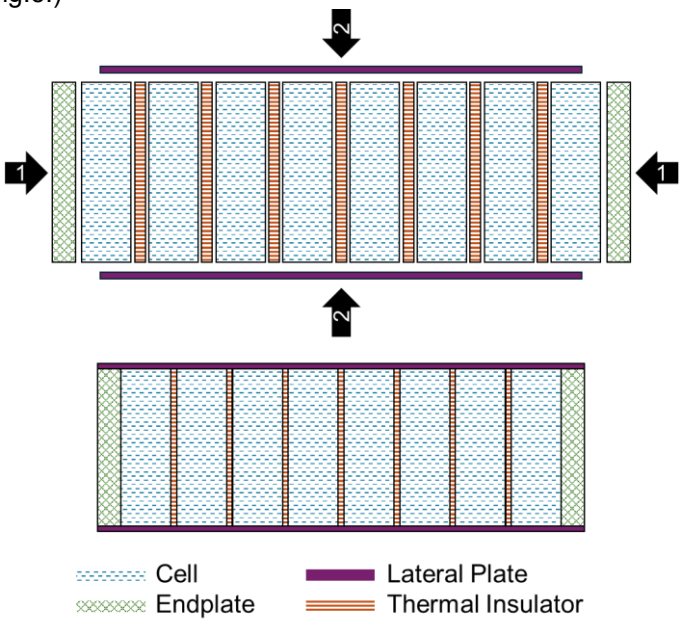

Fig.5: Prismatic-cell based module assembly process – stacking and lateral plate connection phase

As illustrated by Fig.5:, the TIs are components that undergo large amounts of compression during the stacking phase. Therefore, TIs exert pressure on the cell faces once the module is assembled. Furthermore, as the material stress-strain behaviour of a TI is similar to foam materials (Fig.4:), the stiffness significantly varies between its “free-state” and assembled state inside a battery module. These two factors could affect the overall module stiffness for crash simulation purposes.

This section will introduce the general module model used for the overall study and the different TI compression methods investigated in Ansys LS-DYNA® battery module simulations. These are:

- **SURFACE_INTERFERENCE** option in the ***CONTACT** keyword
- **MORTAR** option in the ***CONTACT** keyword
- ***INITIAL_FOAM_REFERENCE_GEOMETRY.**

3.1 Presentation and LS DYNA implementation of methods

3.1.1 Interference contact method

The **SURFACE_INTERFERENCE** option in the ***CONTACT** card is used in order to induce contact forces while removing penetrations from overlapping components at the beginning of an Ansys LS-DYNA® simulation. The basic method is as follows [3]:

- "Standard" Ansys LS-DYNA® nodal penetration check method is switched off (as penetration removal using this method does not induce contact forces).
- **SURFACE_INTERFERENCE** options applies forces over a user defined period of time that eliminates the penetration. A user-defined contact stiffness scale factor is also used throughout this process to calculate the resulting contact forces on the slave and master segments.

All components in the battery module are modelled in their assembled configuration except the TIs which are modelled uncompressed, as illustrated in Fig.6:below:

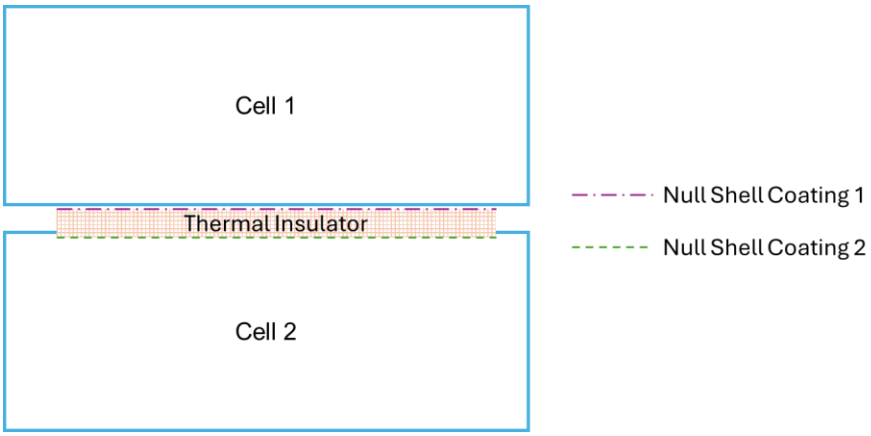

Fig.6: Thermal Insulator to Cell interaction with **SURFACE_INTERFERENCE** *option*

Null shell coating is applied to the TI solid elements in order to manage the interference contact, and the solid TI elements are removed from the global single surface contact with the remaining purpose of providing accurate stress-strain behaviour as per Fig.4:

As can be observed in Fig.6:, the initial TI penetration into the cell can only occurs on a single side of the TI. The null shell elements in Coating 1, where no initial penetration exists, are included in the global single surface contact. This provides added numerical stability during the penetration removal phase. In instances where both TI surfaces were penetrating into the respective adjacent cell cans, and removed by an interference contact, negative volume occurrences were observed.

The null shell elements in Coating 2 are excluded from the global single surface contact, and included in a separate ***CONTACT_SURFACE_TO_SURFACE_INTERFERENCE** keyword. The user provides load curves that define the contact stiffness behaviour, depending on whether transient or dynamic relaxation (DR) methods are used to remove the penetration. Both methods are evaluated in this paper. For the transient method, a single load curve (LCID2) is specified (Fig.7:(a)). This load curve specifies the increase of the contact stiffness from 0 to 100% for a user-defined time during which the penetration is removed, then the contact stiffness is maintained constant for the remainder of the simulation.

SURFACE_INTERFERENCE operates differently when DR is activated. In this case, the ratio between the current and peak kinetic energy is calculated periodically after a user-defined number of cycles. When the ratio falls below a tolerance value, convergence is assumed and the DR run is terminated. The stresses and deformation induced by this process represent the initial state of the component for

subsequent transient simulations. It is therefore essential that the convergence does not occur before the TI has achieved its intended assembled thickness. Fig.7:(b) below highlights the user-defined curve, LCID1, that specifies, similarly to LCID2 for the transient method, the increase in contact stiffness enabling the removal of initial penetration. LCID2 in this case is set constant with a value of 1.0, essentially maintaining the contact stiffness when the transient phase begins after DR.

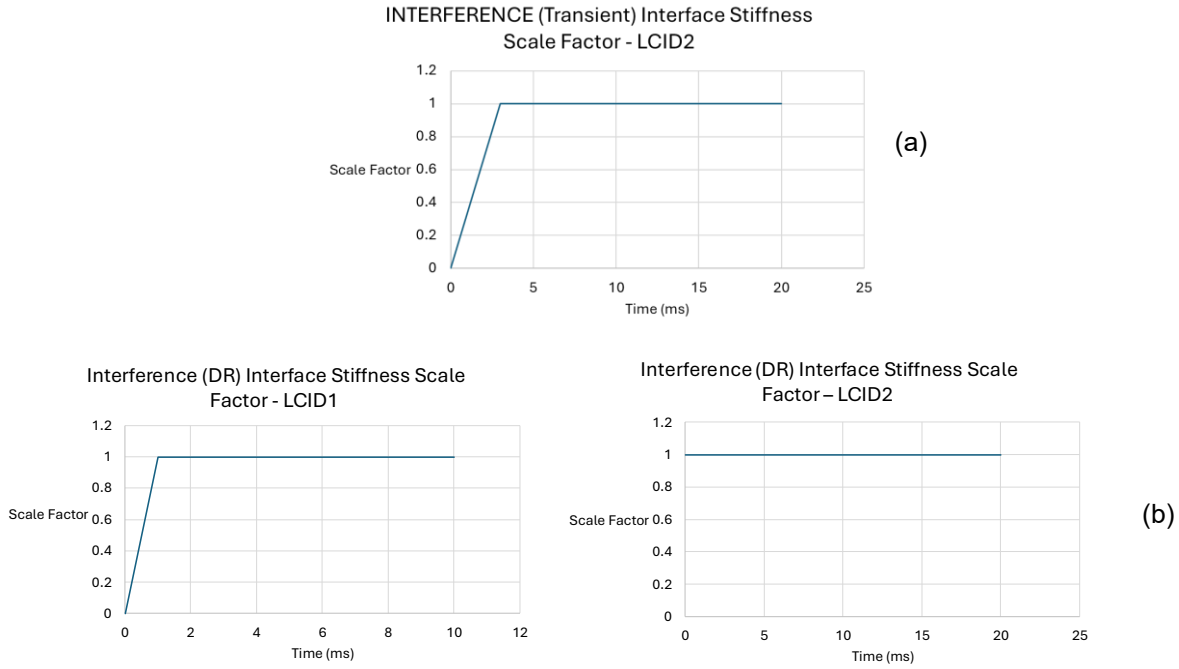

*Fig.7: (a) **SURFACE_INTERFERENCE** (transient) input stiffness scale factor curves (b) **SURFACE_INTERFERENCE** (DR) input stiffness scale factor curves*

The evolution of contact stiffness provided by LCID1 for the DR-based method allows for the correct assembly TI thickness to be reached prior to convergence, as illustrated by Fig.8: below:

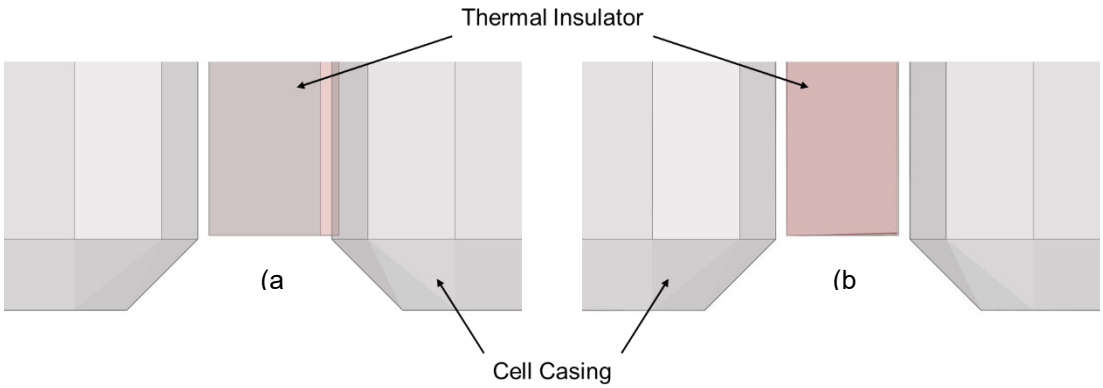

*Fig.8: **SURFACE_INTERFERENCE** with DR (a) original thickness (b) compressed thickness*

Given the removal of standard initial penetration checks by the solver, segment orientation checks are also removed from the process. Therefore, the use of the **SURFACE_INTERFERENCE** option requires the user verify that segment normals are oriented towards each other as illustrated by Fig.9: below.

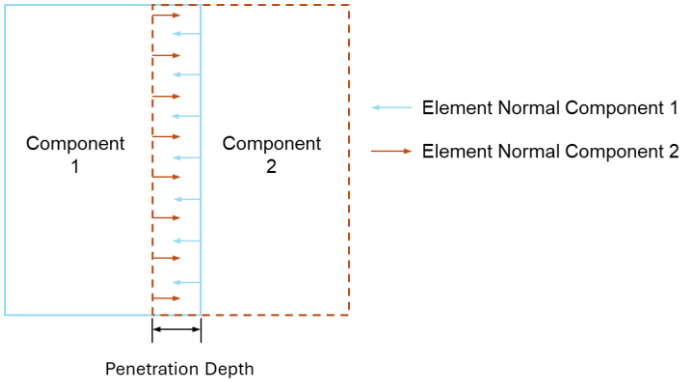

*Fig.9: **SURFACE_INTERFERENCE** contact segment normal orientation requirements*

3.1.2 Mortar contact method

The **MORTAR** option for ***CONTACT** keywords was developed and is typically used for implicit Ansys LS-DYNA® analyses. However, it can also be used for press-fitting or compressed assembly representations via the IGNORE parameter [4]. When set to IGNORE = 4, large penetrations of solid elements are removed by moving, within a user-defined time, the penetrating slave nodes to be coincident with the master surface.

The module configuration and TI starting geometry is as described in Section 3.1.1 and Fig.6:; however, the TI coating differs slightly from Fig.6:. An identical null coating is applied to the TI surface with no initial penetration and remains in the single surface contact. One distinction from the **SURFACE_INTERFERENCE** method is the lack of null shell coating on the penetrating TI surface due to the incompatibility between null shells and the **MORTAR** contact method. The TI solid elements are removed from the single surface contact and used in a ***CONTACT_SURFACE_TO_SURFACE_MORTAR** keyword.

The parameter MPAR1 which governs the removal of penetration is set to 3ms to replicate the setup of the transient **SURFACE_INTERFERENCE** method. An additional parameter MPAR2 is required as it specifies the maximum initial penetration depth and allows the solver to locate the penetrating contact surface and estimate the initial penetration depth [5]. With an initial penetration measured at 0.5mm between the TI and cell casing in the model used for this study, MPAR2 is set to 0.7mm.

3.1.3 Initial foam reference geometry method

The final option evaluated for TI compression initially consists of meshing the entire module, TI included, in its compressed state (Fig.10:). The pre-loading of the TI in this instance is defined through the ***INITIAL_FOAM_REFERENCE_GEOMETRY** keyword, where the user specifies the nodal coordinates of the TI in its uncompressed state. The main requirement at this stage is that the node IDs for the TI parts must match between the standard ***NODE** and ***INITIAL_FOAM_REFERENCE_GEOMETRY** keywords.

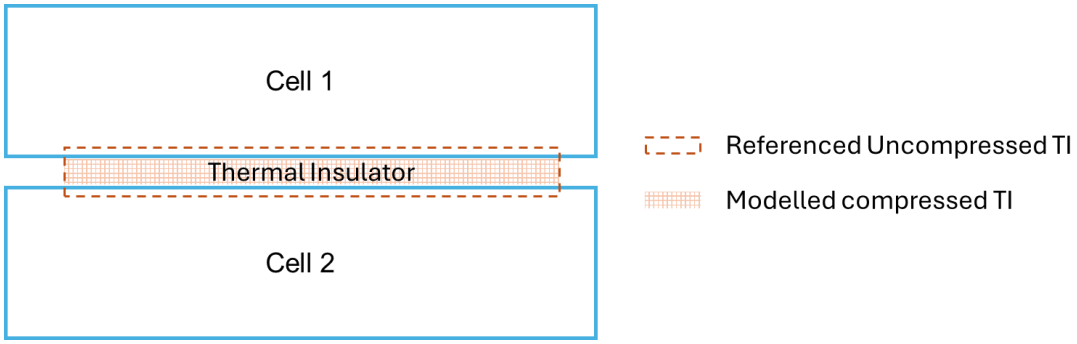

*Fig.10: Thermal Insulator to Cell interaction for **INITIAL_FOAM_REFERENCE_GEOMETRY***

Internal stress is calculated using the deformed (i.e. meshed) and undeformed (i.e. referenced) geometries and associated material stress-strain curve (Fig.4:), defining the compressed components state at the first simulation timestep. The typical behaviour of an unconstrained component would be to return to its referenced state defined in **`*INITIAL_FOAM_REFERENCE_GEOMETRY`** from its meshed state.

In the case of a TI in an assembled module environment, the TI expands as internal stress is released until contact is initiated with the cell casing, providing resistance until an equilibrium is reached.

3.2 Numerical stability evaluation

This section will compare the methods introduced above in terms of their numerical stability and cost. The Ansys LS-DYNA® module model is unconstrained for this particular study, and the stability of each method will be evaluated after a run time of 20ms. Table 1: below summarises for each method the duration of the “pre-loading” phase

Method	**Pre-loading duration (ms)**	**Comments**
`*CONTACT_XXXX_INTERFERENCE` (Transient)	3	Linear removal of contact penetration
`*CONTACT_XXXX_INTERFERENCE` (Dynamic Relaxation)	N/A	As described in Section 3.1.1, DR-based penetration removal is controlled by a convergence tolerance, not a time frame.
`*CONTACT_XXXX_MORTAR`	3	Linear removal of contact penetration
`*INITIAL_FOAM_REFERENCE_GEOMETRY`	0	The internal pressure calculated from the reference geometry is released at the first timestep

Table 1: TI Pre-loading phase duration summary

The following performance criteria are used to compare the behaviour between the methods references in Table 1:

- Contact force between the TI and Cell casing: When the pre-loading phases are completed, the energy stored in the TIs will be released and they will apply pressure on the cell casing faces. Therefore, the amount of pressure applied and the time taken to stabilise will be evaluated.
- Endplate / Lateral Plate weld forces: The pre-loading of the TIs results in pressure applied to the module endplate, connected to each other through the welded lateral plates. The shear forces transferred during pre-loaded will be analysed similarly to the cell casing contact force for the converged force value and the oscillatory behaviour
- CPU Time: The pre-loading methods are applied prior to typical crash simulation profiles such as crush or deceleration loading. Therefore, the additional CPU time required is important to evaluate their viability.

Fig.11: below highlights the contact force evolution between a given TI and adjacent cell face:

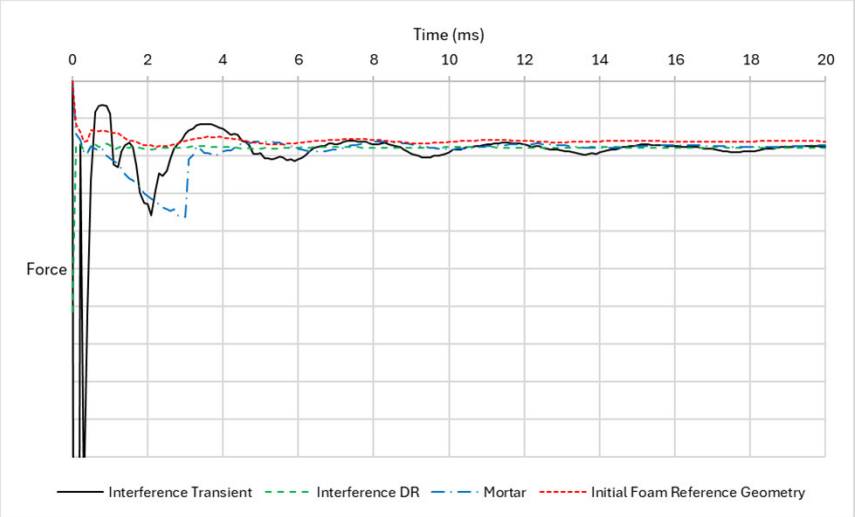

Fig.11: Cell Casing / TI Contact Force during pre-loading

The first notable phenomena observed is the convergence of each method toward a similar value. This highlights that despite the numerical difference between each method, the resulting representativity is similar. However, there is a notable difference in oscillatory behaviour. Assuming the contact force has stabilised by the end of the pre-loading (i.e. after 20ms), the curves are normalised to find the relative percentage difference between the contact force at a given time and the stabilised value using the following equation:

$$Relative\ difference\ (\%) = \frac{F_n - \bar{F}}{\bar{F}} \times 100$$

where F_n is the current contact force and $\bar{F}$ the converged force value. In essence, this provides an indication of when a pre-loading method's oscillatory behaviour has stabilised below an acceptable threshold. For the purposes of this paper, a value of ± 5% deviation from the stabilised force value is used as a threshold. Fig.12: below illustrates the relative difference for each pre-loading method:

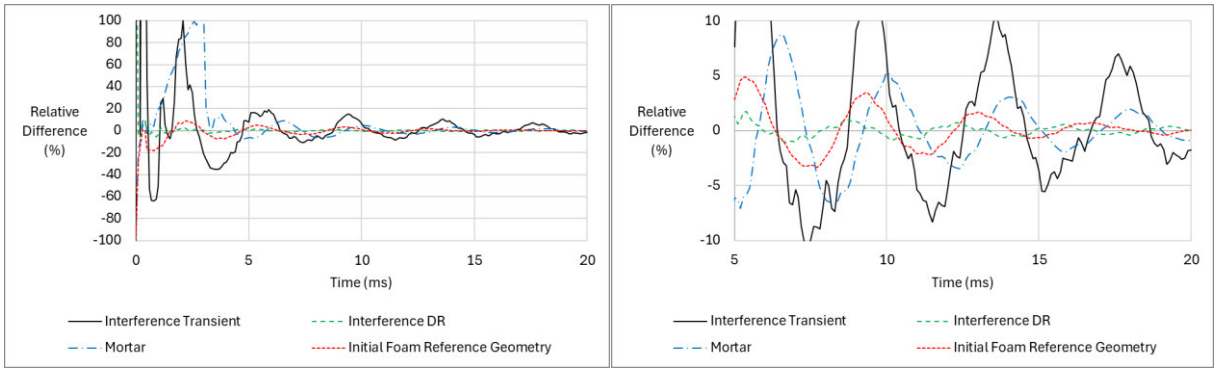

Fig.12: Cell Casing / TI Contact Force relative difference during pre-loading (a) Global overview (b) focus on acceptability criteria

Fig.12: highlights the prolonged oscillation behaviour of the **SURFACE_INTERFERENCE** method using the transient explicit solver compared to the three other methods. Several trends can be observed by truncating the graphs around the acceptability criteria of 5% (Fig.12:(b)). Firstly, the **SURFACE_INTERFERENCE** method using DR has little oscillatory behaviour, with relative differences largely below 5% after 5ms of pre-loading. The ***INITIAL_FOAM_REFERENCE_GEOMETRY** method is also just below the 5% threshold at around 5ms of pre-loading, while the method using **MORTAR** reached

the threshold at approximately 10ms of pre-loading and finally the **SURFACE_INTERFERENCE** method after 17ms on average although peaks above 5% are noticeable.

Similar trends can be observed by evaluating the weld forces between the endplate and the lateral plates (Fig.13: and Fig.14: below)

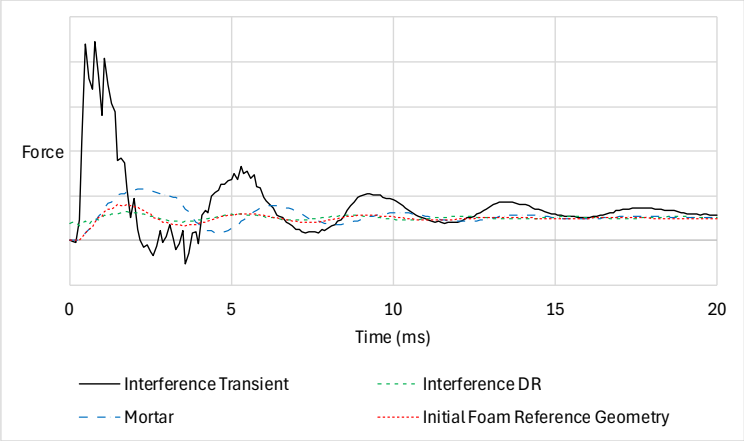

Fig.13: Endplate / Lateral Plate weld shear forces during pre-loading

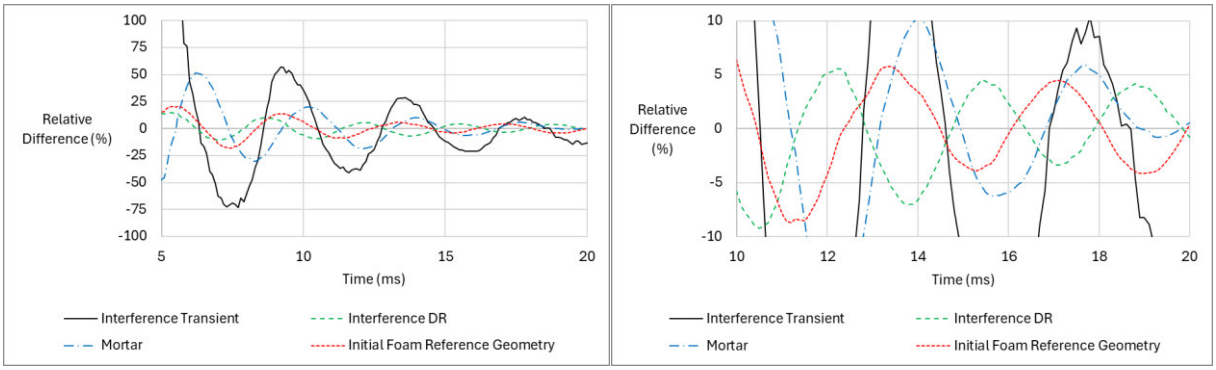

Fig.14: Endplate / Lateral Plate weld shear forces relative difference during pre-loading (a) Global Overview (b) Focus on acceptability criteria

In general, for all methods, the force stabilisation time has increased compared to the cell to TI contact force. Like observed for the cell / TI contact forces, the **SURFACE_INTERFERENCE** method with DR and ***INITIAL_FOAM_REFERENCE_GEOMETRY** methods generally have better oscillation behaviour compared to the **MORTAR** and transient **SURFACE_INTERFERENCE** methods.

Table 2:below summarises the stabilisation of each method for the two performance indicators discussed above, with an indication of the approximate first instance where the peak force values fall within 5% of the converged value

Method	Cell Casing / TI peak force value within 5% of converged value (ms)	Endplate / Lateral Plate peak force value within 5% of converged value (ms)
***CONTACT_XXXX_INTERFERENCE** (Transient)	17	N/A
***CONTACT_XXXX_INTERFERENCE** (Dynamic Relaxation)	< 5	15.5
***CONTACT_XXXX_MORTAR**	9.5	17
***INITIAL_FOAM_REFERENCE_GEOMETRY**	5.5	15

Table 2: Pre-loading methods stabilization summary

SURFACE_INTERFERENCE with DR and ***INITIAL_FOAM_REFERENCE_GEOMETRY** have better stabilisation times compared to the other two methods as highlighted by Table 2:. Considering that the pre-loading methods presented are in addition to typical crash simulation loading scenarios, **SURFACE_INTERFERENCE** and ***INITIAL_FOAM_REFERENCE_GEOMETRY** could therefore require less time before activating additional loading profiles.

As discussed earlier in this section, the CPU time is also important to evaluate any additional costs incurred by each method. Table 3:below summarises the run times for each method for a pre-loading time of 20ms and the CPU increase compared to the fastest method:

Method	Pre-loading CPU time (minutes / seconds)	% CPU time increase compared to lowest
***CONTACT_XXXX_INTERFERENCE** (Transient)	21 mins 41 secs	-
***CONTACT_XXXX_INTERFERENCE** (Dynamic Relaxation)	22 mins 11 secs	2.3
***CONTACT_XXXX_MORTAR**	27 mins 5 secs	25
***INITIAL_FOAM_REFERENCE_GEOMETRY**	24 mins 50 secs	15

Table 3: CPU run times for 20ms TI pre-loading

While all methods are within the same order of magnitude, the **MORTAR** option requires the longest run time, with an additional 25% CPU time compared to the transient **SURFACE_INTERFERENCE** method. Furthermore, as the MORTAR option is maintained for any subsequent crash loading, the CPU requirement difference with the other three methods will further increase.

***INITIAL_FOAM_REFERENCE_GEOMETRY** also requires more CPU time compared to both **SURFACE_INTERFERENCE** methods. However, given the much higher stabilisation time required for the transient variant of the **SURFACE_INTERFERENCE** contact, only the DR option could be considered as effectively requiring less CPU time than using ***INITIAL_FOAM_REFERENCE_GEOMETRY**.

Method	Strengths	Weaknesses
***CONTACT_XXXX_INTERFERENCE** (Transient)	• Least amount of CPU run time…	• Long stabilisation time required • Additional null shell coating and contact keywords needed • Contact segment orientation verification is required
***CONTACT_XXXX_INTERFERENCE** (Dynamic Relaxation)	• Very limited oscillatory behaviour • Very slight CPU increase compared to transient interference method	• Additional null shell coating and contact keywords needed • Contact segment orientation verification is required • Dependency on DR convergence tolerance, risk of early termination before full removal of penetration
***CONTACT_XXXX_MORTAR**	• Lower stabilisation time required compared to transient interference method…	• Noticeably higher oscillation compared to remaining two methods • Separate contact must be defined between TI solid elements and surrounding structural components • Expensive CPU time that is extended after pre-loading
***INITIAL_FOAM_REFERENCE_GEOMETRY**	• Relatively quick stabilisation of oscillations… • No null shell coating or contact keyword creation requirements	• Slight increase in CPU time

Table 4: TI Pre-loading method summary

Based on the summary provided in the above Table 4:, ***INITIAL_FOAM_REFERENCE_GEOMETRY** is selected as the TI pre-loading method for the remainder of this paper due to easier integration into a module environment and good stabilization performance vs CPU time requirements.

3.3 Module crush simulation implementation

In this section, the ***INITIAL_FOAM_REFERENCE_GEOMETRY** TI pre-loading method is evaluated when applied to a module crush scenario to evaluate its influence on overall stiffness and behaviour.

As illustrated in Fig.15: below, the crush scenario selected is a quasi-static half-sphere crush in the module longitudinal direction (X axis in Fig.3:). The half-sphere is 150mm in diameter and modelled using shell elements and a ***MAT_RIGID** material card with standard steel properties. A ***BOUNDARY_PRESCRIBED_MOTION** keyword is applied with a constant velocity of 100mm/s as it allows for a relatively low CPU time while maintaining low inertia effects compared to the module internal energy. This scenario is performed with and without pre-loading for comparative purposes and the simulation terminated after an intrusion of 4mm into the module.

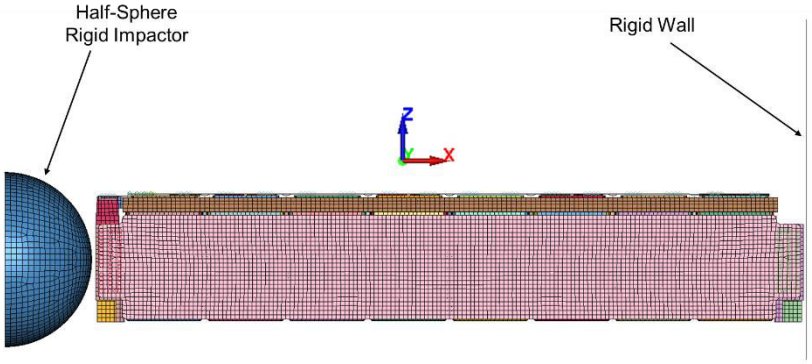

Fig.15: Longitudinal module crush setup

Fig.16: below illustrates the force vs displacement curves for the module crush scenario with and without TI pre-loading implemented. Little change in behaviour is observed and only a 1.5% increase in force at 4mm intrusion is measured with pre-loading applied. This demonstrates that TI compression has a limited effect on the module longitudinal stiffness. As TI compression occurs in the X direction as defined in Fig.15:, it is therefore expected that the influence of pre-loading would be more limited in Y and Z directions.

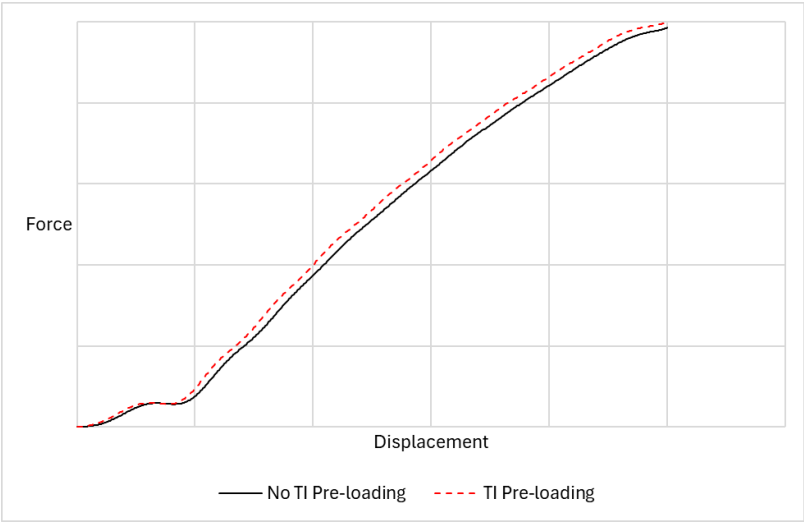

Fig.16: X Crush module reaction force vs displacement with and without TI pre-loading

Even though TI pre-loading did not change module stiffness significantly, for the purposes of more accurate stress state representation within the module and preparing the Ansys LS-DYNA® model for

future multi-physics approaches, TI pre-loading remains a key phenomenon to implement. The effect of TI preloading with the inclusion of cell swelling could be an interesting topic since TIs may reach higher levels of compression resulting in a higher stiffness, thereby contributing to the overall stiffness of the module.

This section has introduced four different pre-loading methodologies to model TI compression during the module assembly process. From a numerical and physical representativity point of view, ***INTIAL_FOAM_REFERENCE_GEOMETRY** was selected to be implemented. Despite the improvements in pre-loaded state representativity (initial pressure in the module and forces in the casing welded connections), the implementation of this phenomena has not resulted in module stiffness improvements targeted in the introduction to this study. The next section will introduce cell swelling behaviour and its numerical implementation with Ansys LS-DYNA® models to evaluate its influence on module stiffness.

4 Cell swelling modelling

4.1 Introduction to swelling concepts

Li-ion cells can undergo swelling such as mechanical swelling of electrodes, generation of gas pressure during initial electrical formation and during charge/discharge cycles, calendaring and ageing. The focus of this paper is on the preloading conditions resulting from electrical formation and charge/discharge cycling at cell level. Furthermore, variations in cell assembly in modules due to dimensional variations will be considered, as well as the TI preloading demonstrated in the previous section. Mechanical swelling can be further categorised as reversible (SOC dependent) and irreversible i.e. State of Health (SOH) dependent. As most safety crash tests are performed one newly built vehicle with fresh batteries, reversible swelling and swelling due to electrical formation are considered critical aspects that need to be modelled to accurately capture module stiffness during crush and mechanical shock conditions.

Cell swelling is modelled using the ***MAT_ADD_THERMAL_EXPANSION** keyword in Ansys LS DYNA®, which is not a direct implementation of swelling as a function of SOC of the cell in R12.2 version. Rather, it is a numerical workaround to adapt thermal expansion as a means of applying cell swelling, correlating a thermal load to the intended cell deformation. This method can be used for both homogeneous and layered approaches to stack modelling [6]. As internal to cell short circuit is not the focus of this paper, a homogeneous modelling of the stack is implemented.

As mentioned in Section 2 of the paper, the cell stack is modelled using ***MAT_MODIFIED_HONEYCOMB,** which enables the swelling to be represented only in the stacking direction of electrodes by defining varying expansion coefficients for each orthogonal direction specified by the material co-ordinate system.

4.2 Cell swelling test and simulation calibration

To characterize the swelling coefficient for thermal expansion applied on the stack, it is necessary to calibrate it using a cell level swelling setup with a module-representative fixture to scale up the swelling behaviour. Fig.17: shows the single cell swelling test setup, containing aluminium plates on each side of the cell with a TI present on one side to represent assembly pressure. The intention of this setup is to represent the cell boundary conditions at module level and to preload the setup at a specific TI compression with the cell at 30% SOC.

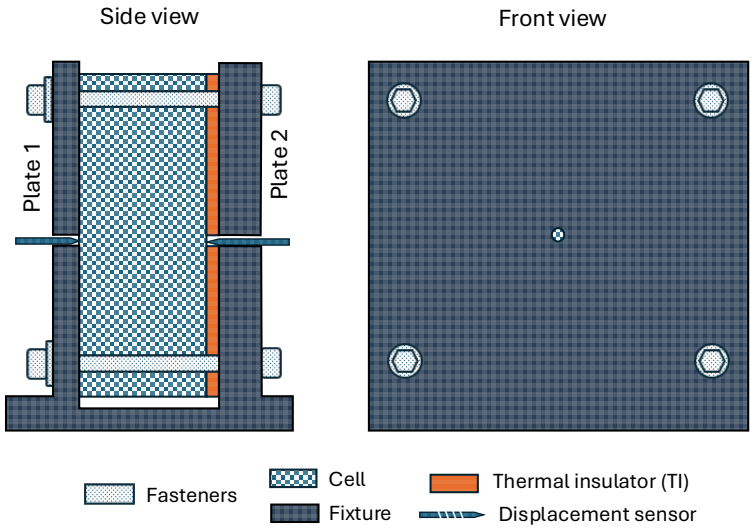

Fig.17: Schematic of cell swelling test setup

A digital twin of this test setup is developed in Ansys LS DYNA®, with the TI modelled using solid elements and using ***INITIAL_FOAM_REFERENCE_GEOMETRY** as discussed in Section 3 to preload the setup along with certain amount of swelling and gas pressure within the cell. Table 5: below summarises the techniques used in Ansys LS DYNA® for modelling the cell swelling setup. The bottom of the fixture is fixed in all 3 translational degrees of freedoms (dofs). The fixture is modelled using solid elements and there are 4 bolts that are connecting the 2 plates which are modelled as 1D beam elements with linear material property.

Preloading conditions	Modeling techniques (keywords)	Preloading time (ms)
TI compression	***INITIAL_FOAM_REFERENCE_GEOMETRY**	The internal pressure calculated from the reference geometry is released at the first timestep
Gas pressure generated inside the cell	***AIRBAG_ADIABATIC_GAS_MODEL**	Airbag model applies pressure at the first timestep
Cell swelling	***MAT_ADD_THERMAL_EXPANSION** ***LOAD_THERMAL_LOAD_CURVE**	After the stabilization of the above 2 preloads, cell swelling is applied over 3 ms and the model is until stabilization of contact force values

Table 5: List of different keywords used to represent preloading conditions in Ansys LS-DYNA® simulation

During the setup of the cell swelling test illustrated in Fig.17:, the assembly force is measured using a force sensor. This total force accounts for TI compression and cell internal loads like gas generation and mechanical swelling of the stack. Simulations are performed with a range of pressures acting on the cell casing because of lack of accurate pressure measurements during assembly of the setup using ***AIRBAG_ADIABATIC_GAS_MODEL** as shown in the equation below:

$$\rho = PSF * P0$$

where ρ is the resulting pressure acting on the control volume, PSF the Pressure Scale Factor and $P0$ the initial pressure (gauge). Cell swelling is modelled using transient loading of the temperature rather than a DR procedure to be compatible with large scale models (pack and vehicle scale) where DR may have stability concerns. Fig.18:below illustrates how the stack expansion is defined in the ***MAT_ADD_THERMAL_EXPANSION** card. To apply expansion only in the electrode stacking direction,

the expansion coefficient is used only on a single parameter, MULTY, and very small values applied to the other parameters, prohibiting expansion in other directions.

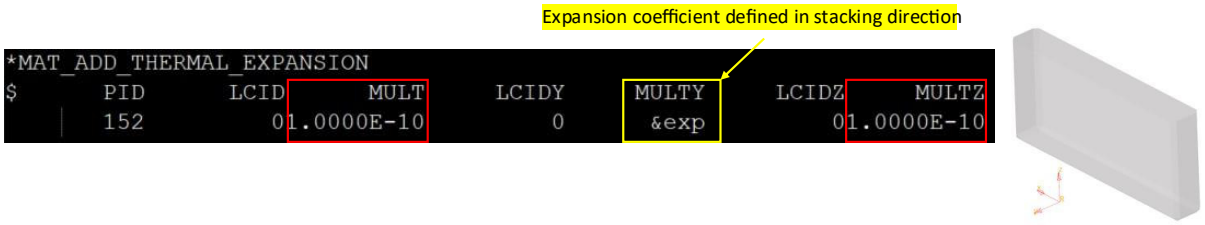

*Fig.18: Description of ***MAT_ADD_THERMAL_EXPANSION** card to simulate cell stack expansion*

To apply the thermal expansion aka stack expansion, the temperature of the stack is modified using the ***LOAD_THERMAL_LOAD_CURVE** keyword as shown in Fig.19:

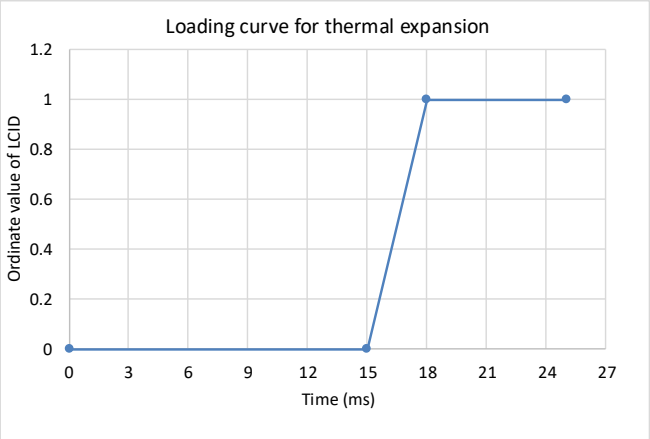

*Fig.19: Load curve defined in ***LOAD_THERMAL_LOAD_CURVE** with offset of 15ms to account for TI preloading and airbag pressure application*

Results of the single cell swelling setup are shown in Fig.20:below. Cell casing displacement (Fig.20:(a)), TI stress after relaxation (Fig.20:(b)), the displacement of the cell faces mid-points (Fig.20:(c)) and the force applied on each plate of the test fixture, calibrated to match with assembly preload measured in the test (Fig.20:(d)) are illustrated.

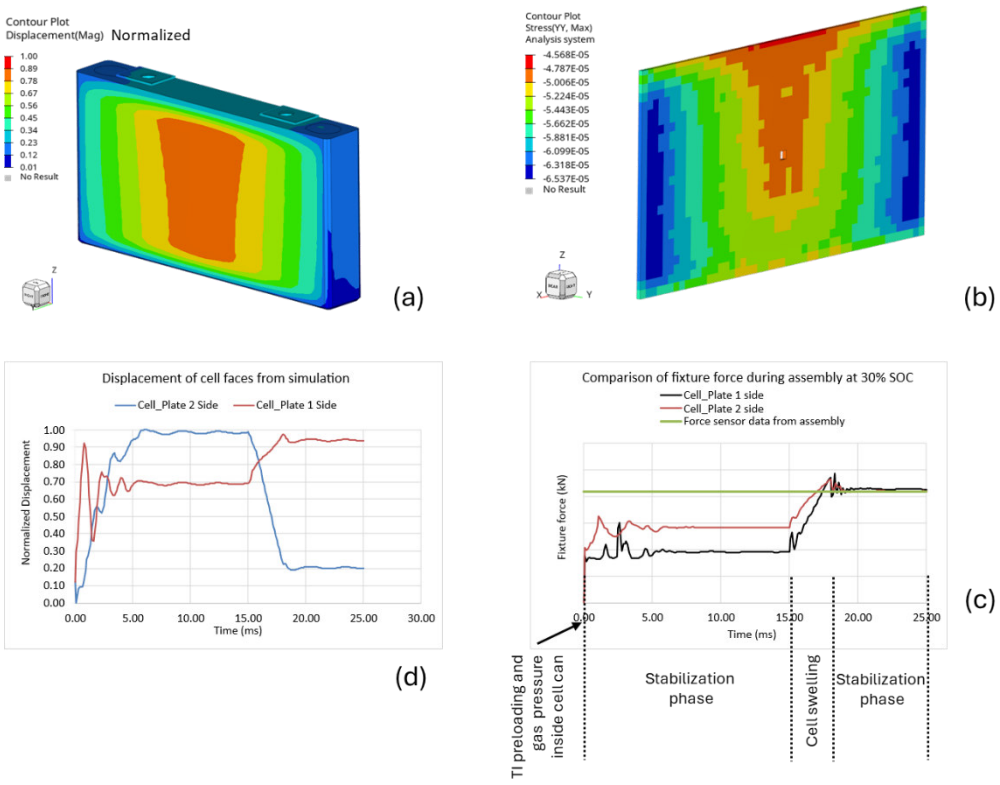

Fig.20: Results representing 30% SOC cell assembly in test fixture Clockwise from the top left, (a) Displacement of cell casing at end of stabilization (25 ms), (b) stress on the TI at end of stabilization (25 ms), (c) Displacement of cell can on each side vs time and (d) Force exerted during assembly on each plate vs time

The swelling coefficient is calibrated based on the load at the plates during assembly and to understand the sensitivity of results with respect to gas pressure within the cell below study is performed from range of pressure from 0 to 1 bar (normalized). Fig.21:indicates the sensitivity of gas pressure for a constant swelling factor on cells and it is evident that up to certain amount of gas pressure from 0 to 0.6 bar (normalized) , there is less influence on the reaction force and based on the assumption that pressure within the cell is not expected to reach higher gas pressure above this limit by reviewing the rate of increase for ageing test (data not published in this paper due to confidentiality) it is concluded that swelling coefficient is more critical to calibrate than the initial gas pressure in the cell.

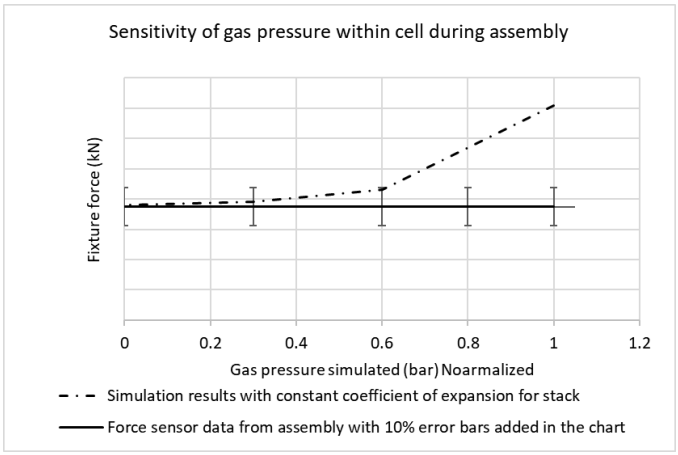

Fig.21: Simulation showing sensitivity of gas pressure for a constant swelling coefficient during assembly

Once the model is calibrated for assembly loads at 30% SOC, next step is to understand the reversible swelling that happens during the cycling of cell. Depending on the profile, max SOC that needs to be

achieved could vary. In this paper, we demonstrate the calibration to achieve 80% SOC. For model validation, there is no force measurement being performed at the testing but the relative displacement of the cells on each side of the setup is used to verify the model predictions. Gas pressure sensor output from the testing helps to understand the change of pressure within the cell and to simplify the representation of reversible swelling in the model, initial gas pressure is assumed to be the total pressure in the cell as shown by the equation below

$$p_{rev} = PSF * (P_0 + \delta p)$$

where p_{rev} = Gas pressure during reversible swelling, P_0 = Initial gas pressure at 30% SOC, δp = change of pressure measured in the test during charging.

Several models were run with different swelling coefficients to arrive at the total displacement of cell measured during the test and simulation results are compared with ratio of displacement on 2 sides of cell to validate the same. As shown in Fig.22: estimated cell swelling on each side of cell is within 10% error as indicated which is indicating the stability and validation of the simulation model.

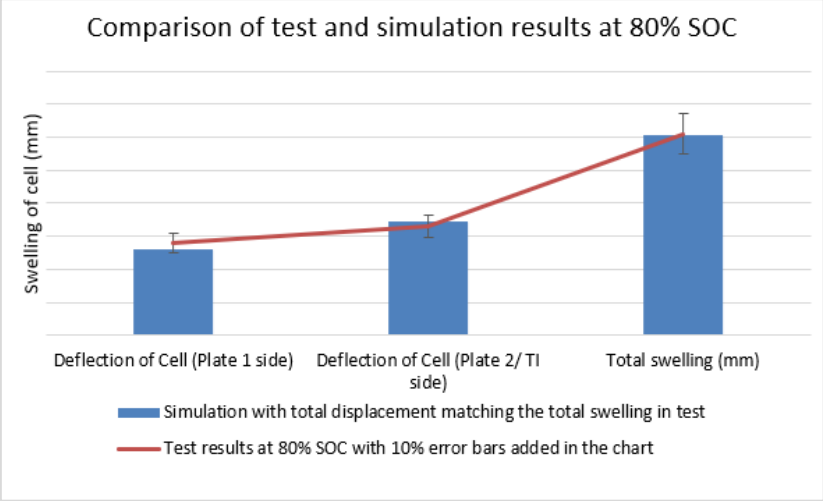

Fig.22: Comparison of swelling of cell in simulation vs test at 80% SOC

4.3 Module swelling implementation

Implementation of preloading in module scale level model is like cell level simulations but can have larger run time and oscillations due to stacking up of cells, TI's. As explained in Section 3 stacking of cells is performed by to required nominal length of the module and thereby exerting compression forces on TI and later constraints on endplate are removed which results in relaxation of endplate and relaxation of loads in the module. Depending on the amplitude of oscillations, additional damping might be introduced but care must be taken to ensure peak loading of stacks are still in good approximation during the simulations.

Cell swelling loads are applied uniformly to all the cells and the load curve for thermal expansion is shown in below Fig.23:

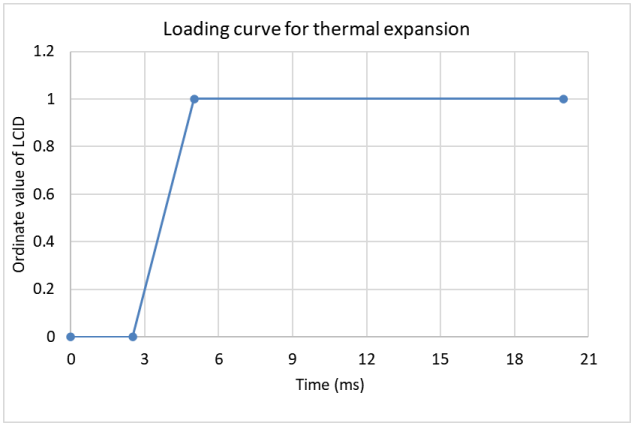

*Fig.23: Load curve defined in *LOAD_THERMAL_LOAD_CURVE with offset of 2.5ms to account for TI preloading and airbag pressure application*

Forces generated on the endplate to the first and last cell in the module is monitored using TIED contact interface between the glue that is present between the endplate to nearby cells in the module. It is to be noted that module boundary conditions are important to calibrate the swelling characteristic of cell because if the module is held constrained in the fixture or in pack, there will be imposed boundary condition, and it will affect the forces on the endplate. For the module results shown below there are no imposed boundary conditions of the module in the direction of swelling but rather for stability of module only Z dir. is constrained to limit any sliding of module due to unbalance in the forces within the module.

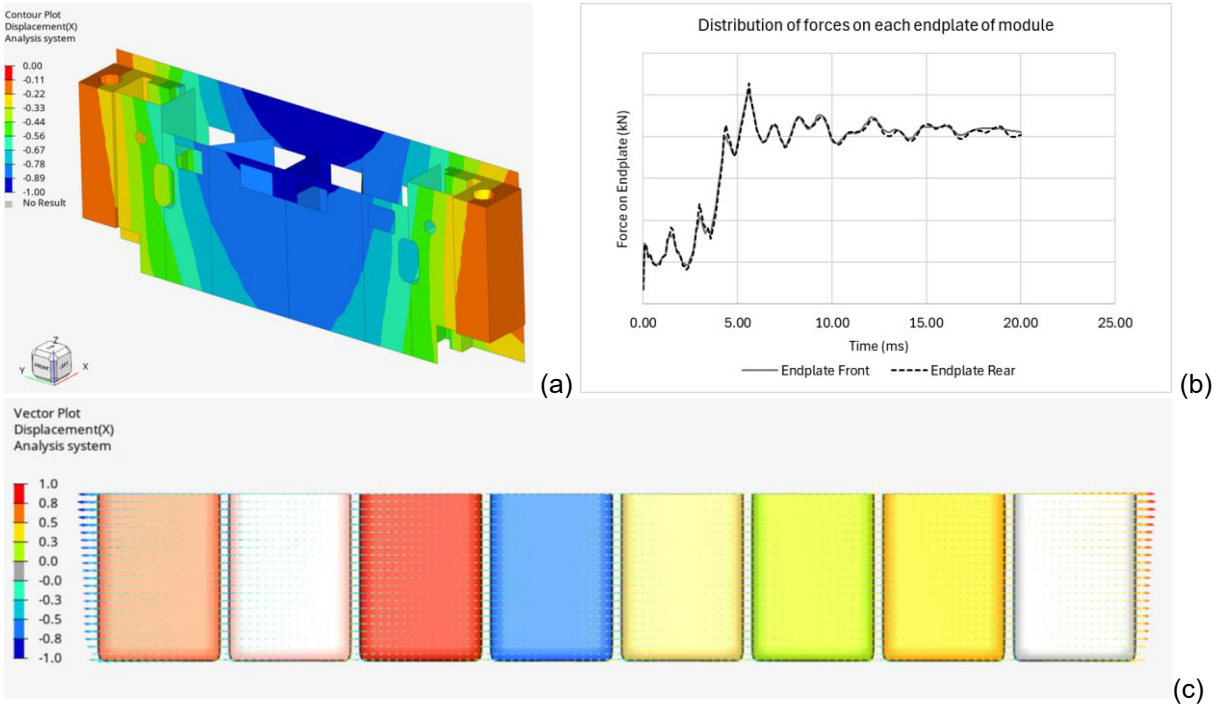

Fig.24: Clockwise from the top left (a) Deflection of front endplate of module at the end of relaxation (20 ms), (b) Force plotted using TIED contact interface at each end of endplate to cell glues, (c) Vector plot of displacement of cell stack to show the distribution of cell swelling in each of the cells at the end of relaxation (20 ms)

As shown in Fig.24: (b) forces on the endplate are stabilized at similar magnitude possible due to symmetric design of module and distribution of forces. It is interesting to observe swelling of cells as shown in (c) which is predominant at end of module primarily resulting from compliance of the end plate which is also confirmed by the displacement contour showing in (a).

5 Numerical validation of module pre-loads

5.1 Module assembly data correlation

Fig.25: below shows the points of endplate for which displacements are measured for an assembled module at 30% and 100% SOC conditions. Point 1-3 captures variation of swelling along the height of the cell stack and Point 4-5 captures variation on the transverse direction of module.

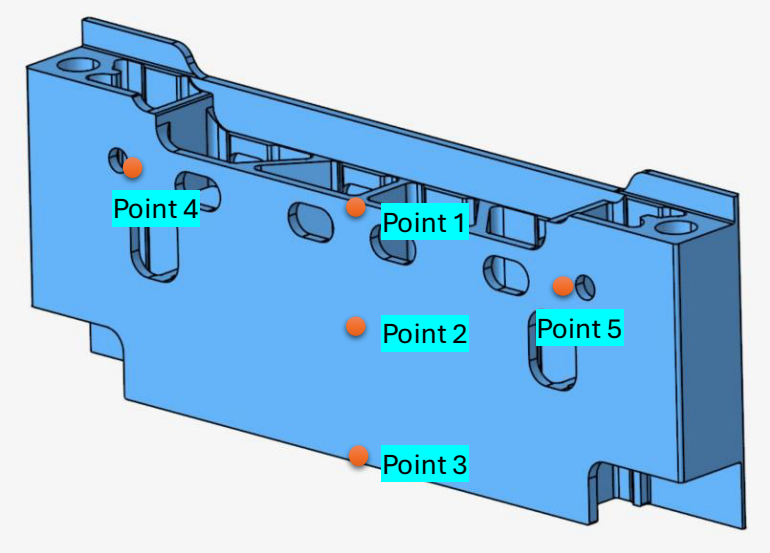

Fig.25: Points on endplate to be correlated with simulation at 30% SOC

For module simulation at 30% SOC, assembly data from the process is obtained to generate the same reaction forces on the endplate to represent the variations that are present in the process. Simulations are performed with min, mean and max preload force measured during assembly or stacking of the cells. Endplate deflections are compared against the spectrum of variation in assembly, and it is found to be correlating very well with the scan data of physical module at 30% SOC as shown in Fig.26:

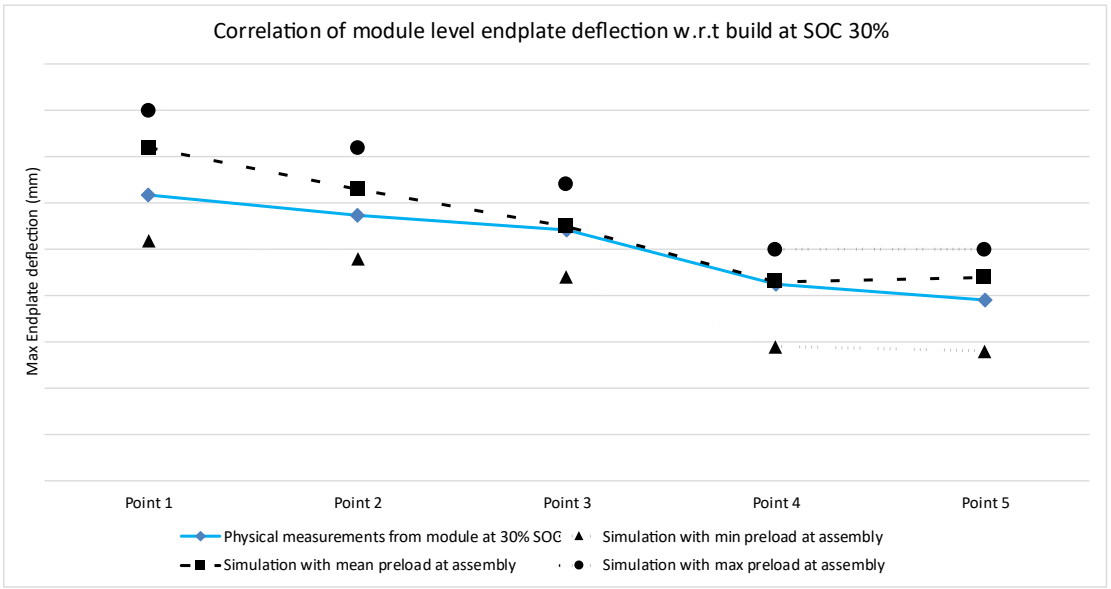

Fig.26: Correlation of endplate displacements at SOC 30% with scan data measurements

To understand the reversible swelling in module environment, another scan is made with physical module at 100 % SOC and it is to be noted that cell level swelling may result in different swelling coefficients if the stiffness of the setup is entirely different from the module level scenario. To calibrate

and understand the endplate deflection at 100% SOC, Point 2 of endplate is chosen which is at the mid point of endplate and swelling coefficients are varied to get close to this deflection data from scan. With that simulation all other points are compared and as indicated in below Fig.27: they all lie close to the scan data within 10% of error bounds on each side. This indicates the uniform reversible swelling applied on the cell stack is a close representation of state of module at 100 % SOC.

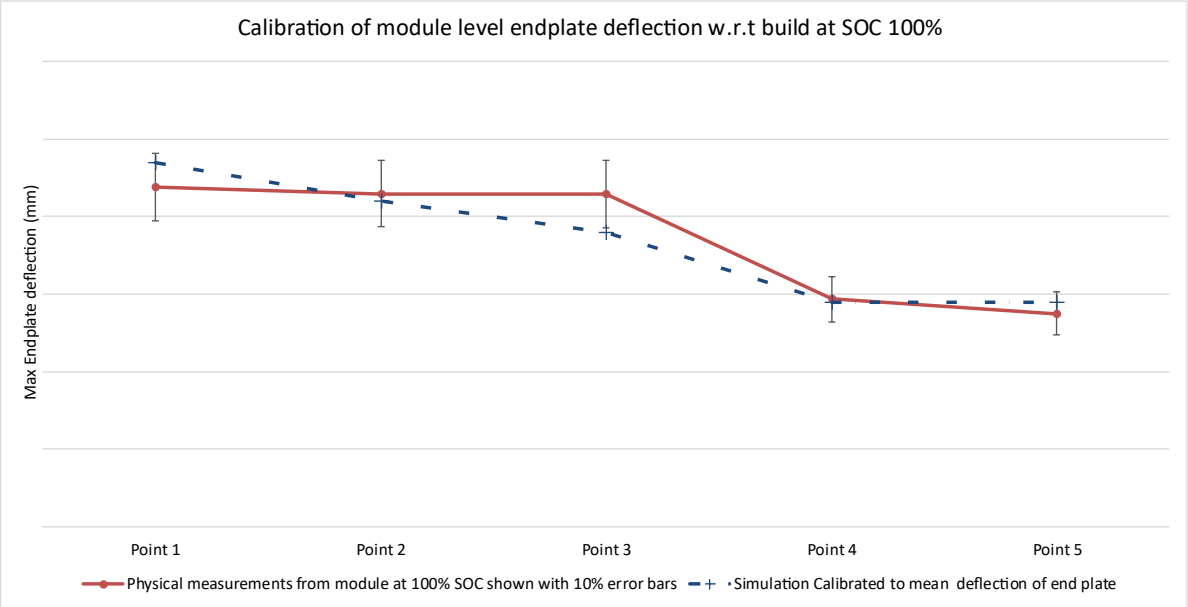

Fig.27: Calibration of SOC 100% data using deflection of endplate at Point 2 and comparing results of other points in endplate

5.2 Module crush test comparison

Since module mechanical tests are usually performed at 100 % SOC to understand the risk of internal/external short and other High Voltage risks, simulation model is also prepared with calibrated module at SOC 100% and performed with 2 directions of crush as shown in Fig.28:below

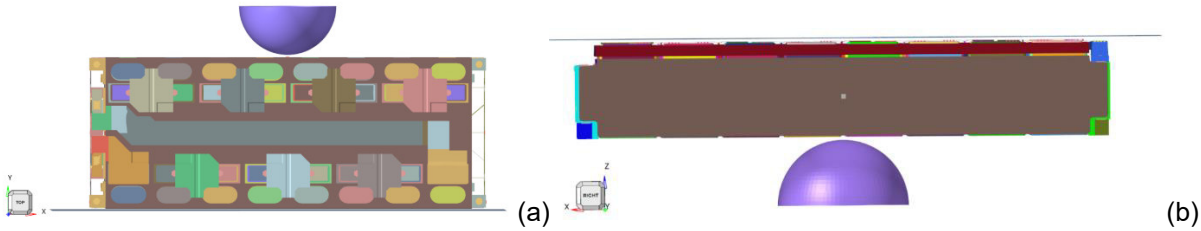

Fig.28: Module crush simulation setup (a) Crush along transverse direction of module in -Y direction (b) Crush along vertical direction in +Z direction

Impactor for the crush loading is hemispherical with radii of 75mm and the loading rate is 50 mm/s to simulate the quasi-static crush test procedure. Reaction force of the impactor is then used to compare the performance of simulation vs test. It is to be noted that top cover of the module is not modelled in the simulation.

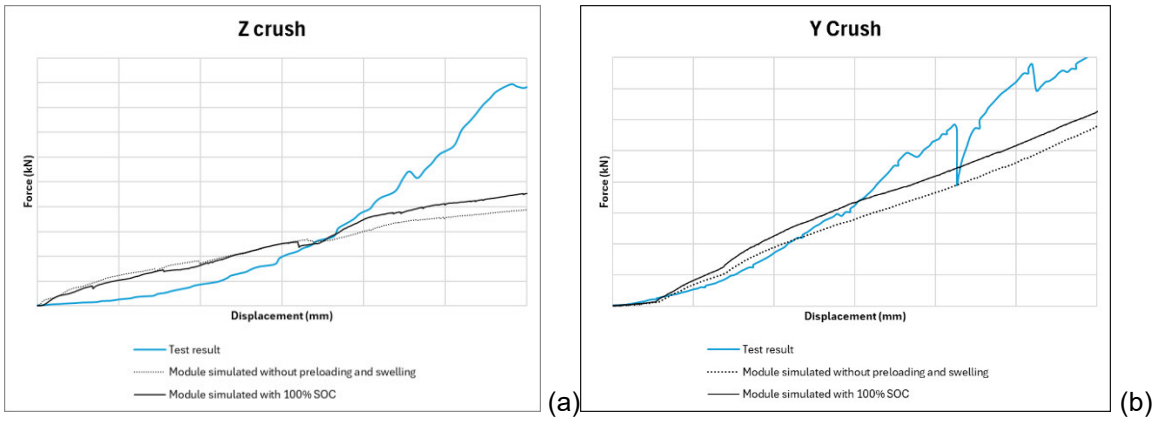

Fig.29: Comparison of crush force vs displacement data for (a) Z crush (b) Y Crush

As it is evident from the correlation of force data between test and simulation that overall stiffness of simulation is not capturing the stiffness from test in both in plane direction (with respect to cell orientation). Adding the preloads on the module helped to improve the correlation but still test shows higher stiffness and this invites more calibration of cell stack material properties at cell level with boundary conditions as per module setup and by adding cell swelling as well. But it is worthwhile to mention with the addition of preload into module simulation, there is an improvement of 15% stiffness in Z direction and 9% stiffness in Y direction.

6 Conclusions and Future work

This paper provides an overview of pre-loading and swelling behaviour implementation with module FEA crash simulation models. Initially, TI assembly compression was implemented, comparing four different methods. With an importance placed on internal module forces stabilisation and computation time, **`*INITIAL_FOAM_REFERENCE_GEOMETRY`** was selected as the best method to represent TI compression at module level. Despite the improvement of local behaviour around TI interfaces, the global effect on module stiffness is limited.

To improve on this initial conclusion and represent all the assembly loads within the module at BOL, formation and reversible swelling behaviour was implemented based on module measurements obtained at 30% and 100% SOC. With the implementation of thermal expansion, the cell/endplate interface forces and module deformations were correlated, albeit only for 30% SOC regarding assembly forces. Cell level investigations were conducted to vary stack expansion in relation to the SOC. This enabled the validation of the numerical techniques to apply TI preloading and cell swelling using **`*MAT_ADD_THERMAL_EXPANSION`** and calibration of the swelling coefficients at various SOC. Gas pressure within the cell did not impact the assembly preloads until certain thresholds, highlighting cell swelling as a critical factor.

While these results are encouraging, the overall impact of TI compression and BOL swelling on module stiffness remains limited. Pre-loading and swelling have an important role in the module stiffness in the initial stages of a module crush. However, increasing levels of intrusion reduces the influence of the pre-loads on module stiffness. Potential avenues of stiffness improvement include, but are not limited to:

- Cell stack refinement: Material characterisation, homogenisation procedures and solid element behaviour improvements.
- Glued interface definitions: Material characterisation for different interface thicknesses
- Test data calibration: Scalability between cell and module level tests (e.g. cell level test with boundary conditions)

Another important limitation, but also indicative of future battery modelling opportunities, is with the use of **`*MAT_ADD_THERMAL_EXPANSION`**. This keyword modifies the thermal properties of the stack, with **`*LOAD_THERMAL_LOAD_CURVE`** applying a change in temperature to the stack. However, as discussed in the introduction, the goal of battery crash models is ultimately to incorporate multi-physics aspects such as thermal propagation or internal short circuit detection. Therefore, ideally no material property modification should be used to induce swelling. The current R16 version of Ansys LS DYNA® has

introduced keywords for tackling this issue, with a thermal independent expansion coefficient and loading applied using **`*MAT_ADD_EXTVAR_EXPANSION`** and **`*LOAD_EXTERNAL_VARIABLE`** respectively. The evaluation and implementation of these keywords will form the basis of future work on cell swelling implementation.

Finally, BOL reversible swelling has been one of the main focuses of this paper. However, ageing mechanisms are also key considerations for module swelling, with gas generation resulting in increasing amounts of module deformations as a function of the number of cycles (irreversible swelling). These phenomena will be important to characterise and implement for future crash simulation models.

7 Acknowledgments

The authors of this paper would like to appreciate and recognise the exceptional support and technical discussions from ANSYS team members especially Pierre Glay, Raphael Heiniger and David Poulard which helped us to constantly improve, adapt new modelling practices and ensure adequate checks are employed for validating simulation models.

The authors would also like to extend their warm thanks to different ACC team members for providing scanned data of the module, sharing crush test results etc. Special mention to Camille Leducq and Philippe Desprez for their invaluable feedback and guidance in writing this paper.

8 References

[1] European Automobile Manufacturers' Association (ACEA), "New Car Registrations, European Union", Press Release, June 2025

[2] Rujian Fu, Meng Xiao, Song-Yul Choe, Modeling, validation and analysis of mechanical stress generation and dimension changes of a pouch type high power Li-ion battery, Journal of Power Sources, Volume 224, 2013, Pages 211-224,ISSN 0378-7753, https://doi.org/10.1016/j.jpowsour.2012.09.096.

[3] Bala,S: "Modeling Press-Fit Conditions to Include Initial Stresses" https://blog.d3view.com/modeling-press-fit-conditions-to-include-initial-stresses/, December 2006

[4] Borrvall, T: "Mortar Contact for Implicit Analysis", 11th LS-DYNA Forum, Ulm, 9-10 October, 2012

[5] LSTC, "LS-DYNA Keyword User's Manual Volume I R12", July, 2012

[6] Höschele, P.; Ellersdorfer, C. Implementing Reversible Swelling into the Numerical Model of a Lithium-Ion Pouch Cell for Short Circuit Prediction. *Batteries* **2023**, *9*, 417. https://doi.org/10.3390/batteries9080417